Assessing soil erosion risk in a peri-urban catchment of the Lake Victoria basin

Gyaviira Ssewankambo[1] · Isa Kabenge[1] · Prossie Nakawuka[1] · Joshua Wanyama[1] · Ahamada Zziwa[1] · Yazidhi Bamutaze[2] · David Gwapedza[3] · Carolyn Tally Palmer[3] · Jane Tanner[3] · Sukhmani Mantel[3] · Bezaye Tessema[4]

Abstract

Soil erosion and sedimentation contribute to deteriorating water quality, adverse alterations in basin hydrology and overall ecosystem biogeochemistry. Thus, understanding soil erosion patterns in catchments is critical for conservation planning. This study was conducted in a peri-urban Inner Murchison Bay (IMB) catchment on the northern shores of Lake Victoria since most soil erosion studies in Sub-Saharan Africa have been focused on rural landscapes. The study sought to identify sediment sources by mapping erosion hotspots using the revised universal soil loss equation (RUSLE) model in appendage with field walks. RUSLE model was built in ArcGIS 10.5 software with factors including: rainfall erosivity, soil erodibility, slope length and steepness, land cover and support practices. The model was run, producing an erosion risk map and field assessments conducted to ground-truth findings and identify other hotspots. The percentage areas for RUSLE modelled erosion rates were: 66.8% for 0–2 t ha^{-1} year^{-1}; 10.8% for 2–5 t ha^{-1} year^{-1}; 10.1% for 5–10 t ha^{-1} year^{-1}; 9% for 10–50 t ha^{-1} year^{-1} and 3.3% for 50–100 t ha^{-1} year^{-1}. Average erosion risk was 7 t ha^{-1} year^{-1} and the total watershed erosion risk was 197,400 t year^{-1}, with croplands and steep areas (slope factor > 20) as the major hotspots (> 5 t ha^{-1} year^{-1}). Field walks revealed exposed soils, marrum (gravel) roads and unlined drainage channels as other sediment sources. This study provided the first assessment of erosion risk in this peri-urban catchment, to serve as a basis for identifying mitigation priorities. It is recommended that tailored soil and water conservation measures be integrated into physical planning, focusing on identified non-conventional hotspots to ameliorate sediment pollution in Lake Victoria.

Keywords Land use land cover · Inner Murchison Bay catchment · Geographical information system · RUSLE

Introduction

Soil erosion poses enormous threats to natural ecosystems and livelihoods worldwide because of its adverse in-situ and ex-situ consequences (FAO 2019; Bamutaze et al. 2021). The UN's Food and Agricultural Organization (FAO) reports that soil erosion is escalating above tolerable thresholds in diverse geographic settings (FAO 2019). Approximately 30% of the planet's land is severely degraded, with soil erosion widely known as the eminent cause of the debacle (UNCCD 2017). Estimates elucidate annual soil losses at global scales with enormous magnitudes ranging between 24 and 35.9 Petagram (Pg)/year (UNCCD 2017). Globally, soil erosion adversely affects terrestrial ecosystems, sometimes triggering gullying (Islam et al. 2020) and the subsequent land degradation posing an important threat to the environment (Islam et al. 2020; Bekele and Gemi, 2021). Various international development agendas are targeting addressing such threats posed on the world ecosystems including the Sustainable Development Goal (SDG) 15 of the United Nations Global Development Agenda 2030, which advocates for life on Land, aiming at the protection, restoration and sustainable management of terrestrial ecosystems (UN 2016). Regardless of water being the world's most valuable

✉ Gyaviira Ssewankambo
  gyaviirassewankambo@gmail.com

1 Department of Agricultural and Biosystems Engineering, Makerere University, P.O Box 7062, Kampala, Uganda

2 Department of Geography, Geo-Informatics and Climate Sciences, Makerere University, P.O Box 7062, Kampala, Uganda

3 Institute for Water Research, Rhodes University, P.O. Box 94, Makhanda, Eastern Cape, South Africa

4 Water and Land Resource Centre, Addis Ababa University, P.O. Box 1176, Addis Ababa, Ethiopia

asset (Clothier, 2015), aquatic ecosystems can be detrimentally impacted by erosion as the eroded sediments impair the water quality (Karamage et al. 2017), further jeopardizing the integrity of the earth's natural systems (UNCCD 2017; Bamutaze et al. 2021).

Lake Victoria is the biggest natural water resource in East Africa, serving diverse roles, from fishing, navigation, eco-conservation to supplying fresh water for various purposes such as irrigation, industrial use and domestic use. According to the African Great Lakes Initiative, the Lake Victoria basin population in 2019 was over 40 million people, with a population growth rate of 3.5% per year, one of the highest rates in the world (AGLI 2020). The gigantic water body has suffered deteriorating water quality attributed mainly to human factors (Bongomin 2011; MWE 2018; Kolding et al. 2014). The water quality has been impaired by nutrient and sediment inputs into the lake, a manifestation of degradation in its catchment (Banadda et al. 2009; MWE 2018). The lake's ecological health has been adversely affected by the rapidly increasing human population in the catchment, clearance of natural vegetation, and emissions of untreated effluent (Banadda et al. 2009). With the country's population projected over 104 million by 2050, this explosion is poised to pose enormous pressure on natural resources, augmenting the risk of soil erosion by water if inadequate conservation practices are applied (Karamage et al. 2017).

The Murchison Bay, consisting of the inner Bay and the outer Bay, is located on the northern shores of Lake Victoria in Uganda. It is the primary water source for Kampala, the Capital City of Uganda, in addition to being the recipient of the runoff and discharged wastewater from the city (Banadda et al. 2009; World Bank 2015). The IMB is suffering from deteriorating water quality and increasing sedimentation (Bongomin 2011; Kayima et al. 2010; Banadda et al. 2009; Akurut et al. 2017; MWE 2018), attributed to both point and non-point pollution sources in its catchment. Even in minute amounts, sediment-adsorbed pollutants such as heavy metals pose grave ecological and human health concerns (Jaishankar et al. 2014; Sankhla et al. 2019; Huang et al. 2020). The pollution impacts are visible in the drainage network and the lake, as evidenced by the frequent algal blooms in Murchison Bay (Ssebiyonga et al. 2013; Haande et al. 2011). As a result, the treatment cost of potable water has increased (World Bank 2015) and the Murchison Bay aquatic ecosystem is at the peril of adverse pollution effects (Lake Victoria Environmental Management Project 2005; Tebandeke et al. 2020). The IMB catchment has two major factions; the eastern, primarily rural, and the western, predominantly semi-urban. Though several studies reckon urban areas as non-erodible zones (Karamage et al. 2017), there is evidence of soaring sediment yields and alarming sedimentation levels, especially in the western Bay (Banadda et al. 2009; MWE 2018). For instance, the sediment yield of only

the Nakivubo sub-catchment of IMB was estimated at a rate of 26.5 t ha^{-1} year^{-1} and 26.4 t ha^{-1} year^{-1} for years 1995 and 2003, respectively (Anaba et al. 2017). There has been a significant loss of forest, wetland and other natural vegetation covers in the catchment due to anthropogenic activities (Anaba et al. 2017) with statistics showing declining forest cover in the Bay from 1274 ha (31%) in 1995 to 569 ha (14%) in 2003 (Anaba et al. 2017). The trend has been worse in recent decades making the catchment more prone to soil erosion and depriving the Bay of its natural buffering effect (Banadda et al. 2009; MWE 2018).

Erosion risk assessments and application of RUSLE in peri-urban and urban catchments have been understudied globally (Shikangalah et al. 2016; Marondedze and Schütt 2020), with urban settings often regarded as non-erodible zones (Karamage et al. 2017). Nonetheless, practically there are complex detachment and sediment transport mechanisms, attributed to the portions of built-up area and the large runoff volumes which trigger erosion and sediment transport within such catchments (Marondedze and Schütt 2020). Similarly in the IMB catchment, there has been no sufficient information on erosion hotspots, with systematic soil erosion assessments lacking in the catchment. However, the development and implementation of soil and water conservation (SWC) measures require a foundation of knowledge and the understanding of soil erosion risk (Bamutaze et al. 2021). Erosion risk assessments serve as a basis to give key insights for the design of appropriate interventions and environmental risk management (Almasalmeh et al. 2022). Thus potential erosion hotspots, which are zones with a high potential to contribute to the overall erosion from the catchment (Karamage et al. 2017), needed to be mapped and their potential erosion rates envisaged. To bridge existing knowledge gaps, the contribution from this research is therefore the assessment of the spatial patterns of erosion risk and identification of erosion hotspots in the IMB catchment to lay a knowledge base for tailored mitigation and conservation measures in this peri-urban catchment to ameliorate sediment pollution into Lake Victoria.

Materials and methods

Description of the study area

The study was for the Inner Murchison Bay (IMB) catchment, located on the northern shores of Lake Victoria, with a size of 282 km^2 with drainage basins (sub-catchments): Nakivubo (40 km^2) in the northwest, Kansanga (15.9 km^2) and Ggaba (Kyetinda) (7.0 km^2) in the west, Kinawataka (35.9 km^2) and Portbell (2.3 km^2) in the north, Namanve (86.7 km^2) in the northeast, Nakiboga (17.5 km^2) and Zirimiti (78.3 km^2) in the East (Fig. 1). The IMB is a
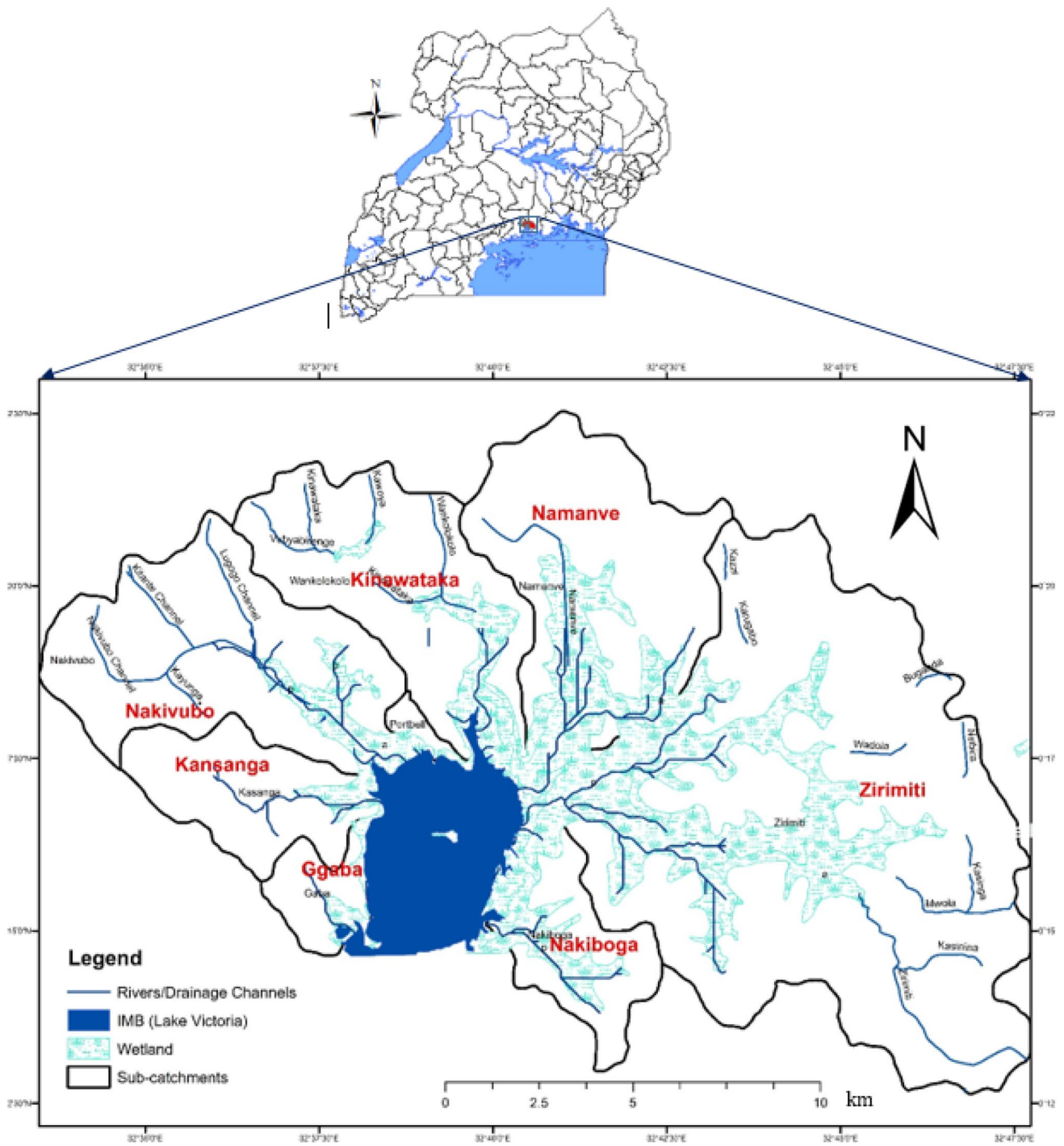
Fig. 1 Map showing the location IMB catchment in Uganda

semi-enclosed small water body of the main Lake Victoria with an area of 18.4 km² and length of 5.6 km (Fig. 1).

Mapping erosion hot spots in the catchment using the RUSLE model

Revised universal soil loss equation (RUSLE) (Renard et al. 1997) was used to estimate erosion risk and the spatial distribution of the erosion hotspots within the IMB catchment. RUSLE model was built in a GIS environment

using ArcGIS 10.5 software and a GISUS-M plugin (Oliveira 2015), focusing on several factors that influence erosion in the catchment. These included: land use/cover, soil data (soil type), topography (DEM), erosion control practices and rainfall data. The RUSLE model was run, producing a sediment hotspot map for the entire IMB catchment. This model was selected because of its minimal data requirements making it more suitable for data-scarce regions (Tamene et al. 2017) like the IMB catchment. The RUSLE model is described in Eq. 1 (Renard et al. 1997):

$$A = R \times K \times LS \times C \times P, \tag{1}$$

where A = estimated average soil loss in t ha^{-1} year^{-1}; R = rainfall erosivity factor (MJ mm ha^{-1} h^{-1} yr^{-1}); K = soil erodibility index (t ha h ha^{-1} MJ^{-1} mm^{-1}); L = slope length factor (dimensionless); S = slope steepness factor (dimensionless); C = land use/cover factor (dimensionless) and P = conservation/management factor (dimensionless).

The RUSLE parameters in Eq. 1 were computed using the input datasets in the ArcGIS software environment. GIS layers for all the contributing factors were generated and then the Raster Calculator in ArcGIS 10.5 software was deployed in computing the RUSLE model to produce the erosion hotspot map for the entire IMB catchment (Fig. 2).

Rainfall erosivity factor (*R*)

R-factor is a key parameter for soil erosion studies and represents the erosive nature of rainfall for a given geographical location using the amount of rainfall and its intensity as inputs (Mekonnen and Melesse 2011). The general formula (Eq. 2) for computing rainfall erosivity factor R that was proposed by Wischmeier and Smith (1978) is:

$$R = \frac{EI_{30}}{1000}, \tag{2}$$

where R = rainfall erosivity factor, E = rainfall kinetic energy (J m^{-3}) and I_{30} = 30 min rainfall intensity (mm h^{-1}). Estimating the R-factor using the above equation required average kinetic energy intensity (EI) values for at least 20 years. However, that data was unavailable for IMB catchment. Instead, R was estimated with an alternative equation proposed by Hurni (1985) and commonly used in studies in East Africa and the Nile basin (Tamene and Le 2015; Njiru et al. 2018; Eniyew et al. 2021; Tsegaye and Bharti 2021; Jothimani et al. 2022) (Eq. 3).

$$R = 0.562 \times P - 8.12, \tag{3}$$

where P is the long-term mean annual precipitation. In this computation, 39 years of CHIRPS rainfall data were downloaded from the CHIRPS website (https://www.chc.ucsb.edu) to produce the mean annual rainfall map in Fig. 3, with values ranging between 1198 to 1570 mm.
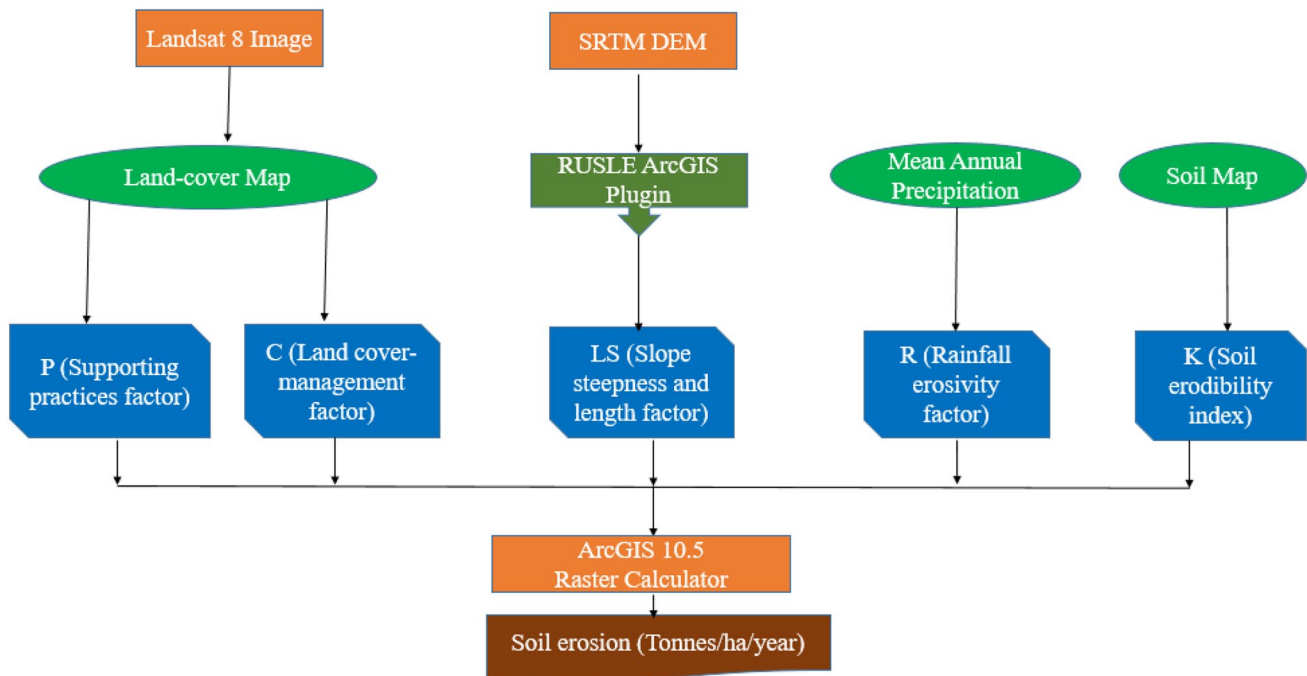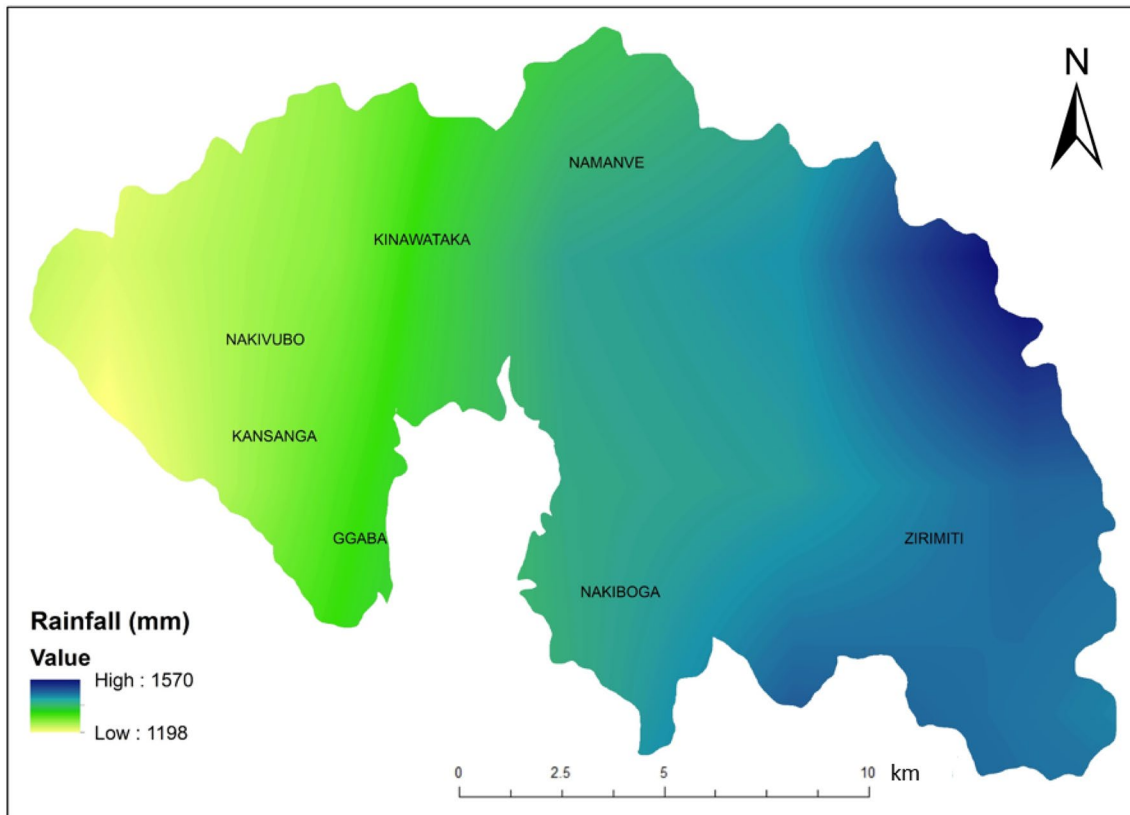

Fig. 2 Schematic layout of the procedure for assessing erosion risk using RUSLE model

Fig. 3 IMB catchment mean annual rainfall for 39 years (1980–2019)

Soil erodibility factor (*K*)

K-factor is a quantitative description and measure of the susceptibility of soil particles to detachment and transport by rainfall and runoff (Karamage et al. 2017). The contributing soil properties for the *K* value include soil structure, texture, organic matter and permeability. Global FAO soil datasets were downloaded from the FAO website (https://data.aps.fao.org/map/catalog/), where the IMB catchment soils were extracted for use in this study (Fig. 4). The *K*-factor for the IMB catchment was computed from FAO soil data using Eq. 4 (Wang et al. 2021).

$$K = f_{csand} \times f_{cl-si} \times f_{orgc} \times f_{hisand}. \tag{4}$$

With ms, msilt, mc and orgc the percentage (%) compositions of sand, silt, clay and organic carbon, respectively. The factors in Eq. 4 are described as:

f_{csand} factor; gives low soil erodibility factors for soils with high coarse sand contents and high values for soils with little sand.

$$f_{csand} = \left(0.2 + 0.3 \times \exp\left[-0.256 \times ms \times \left(1 - \frac{msilt}{100} \right) \right] \right) \tag{5}$$

f_{cl-si} factor; gives low soil erodibility factors for soils with high clay to silt ratios.

$$f_{cl-si} = \left(\frac{msilt}{mc + msilt} \right) \tag{6}$$

f_{orgc} factor; that reduces soil erodibility for soils with high organic carbon content.

$$f_{orgc} = \left(1 - \frac{0.0256 \times orgC}{orgC + \exp\left[3.72 - 2.95 \times orgC \right]} \right) \tag{7}$$

f_{hisand} factor; reduces soil erodibility for soils with extremely high sand contents.

$$f_{hisand} = \left(1 - \frac{0.7 \times \left(1 - \frac{ms}{100} \right)}{\left(1 - \frac{ms}{100} \right) + \exp\left[-5.51 + 22.9 \times \left(1 - \frac{ms}{100} \right) \right]} \right) \tag{8}$$

The *K*-factors were multiplied with 0.1317 value to convert the *K*-factor from the American system to the metric system unity/International System of Unit (Karamage et al. 2017; Bamutaze et al. 2021). The primary soil types in the catchment were gleysols and ferralsols (acric and lixic).

Fig. 4 **a** Map of major soil types in the IMB catchment. **b** Map of IMB catchment DEM
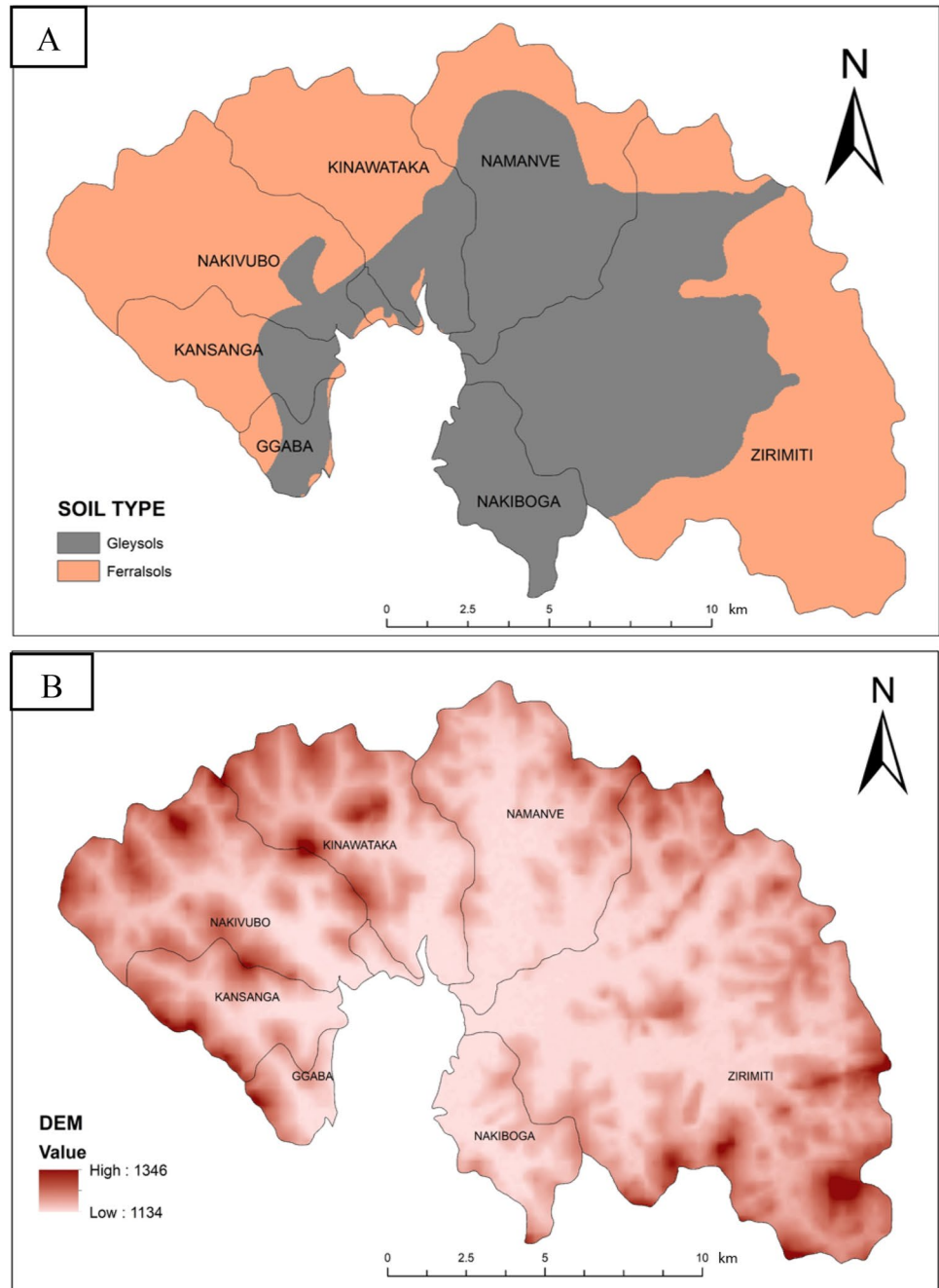
Soil erodibility values were categorized as per IWR (2002) classes (Table 1).

Slope factor (LS)

Soil erosion is highly correlated with slope and therefore increases rapidly with slope (David 1988). L stands for the effect of slope length on soil erosion. It is the ratio of field soil loss to the corresponding soil loss from a 22.13 m length on the same soil type (Uddin et al. 2016). The *S* represents the effect of slope steepness on erosion (Uddin

Table 1 Thresholds for categorization of soil erodibility (*K*-factor) as per IWR (2002)

No.	Erodibility class	Threshold values	Predominant soil
1	Low *K* values	0.006585–0.019755	Clay soils
2	Low *K* values	0.006585–0.02634	Course textured soils
3	Moderate *K* values	0.02634–0.05268	Medium textured soils
4	High *K* value	> 0.05268	Soils with high silt content

Table 2 Land use and land cover (LULC) descriptions and their averaged *C* values

Cover type	Description	Averaged *C* value	Sources
Built-up	Industrial, Central business districts and residential areas with a lot of impervious surfaces and low vegetation (<25% green)	0.035	Eisenberg and Fabrice (2020), Eniyew et al. (2021), Ligonja and Shrestha (2013), Marondedze and Schütt (2020)
Semi-built up	Built suburbs with medium vegetation cover (25–50% green)	0.11	Eisenberg and Fabrice (2020), Marondedze and Schütt (2020)
Forest area	Evergreen natural and artificial forests	0.011	Eisenberg and Fabrice (2020), Eniyew et al. (2021), Ligonja and Shrestha et al. (2013), Tsegaye and Bharti (2021)
Cropland	Cultivated land	0.3	Eisenberg and Fabrice (2020), Bamutaze et al. (2021), Marondedze and Schütt (2020)
Bare surfaces	Exposed/unpaved soils with no vegetation cover	1	Eniyew et al. (2021), Ligonja and Shrestha et al. (2013)
Open water	Lakes, rivers and reservoirs	0	Ganasri and Ramesh (2016), Wang et al. (2016)
Wetlands	Swamps	0	Armour and Lait (2014), Rozos et al. (2013)

et al. 2016). An SRTM DEM (Fig. 4) was downloaded from the USGS website (https://earthexplorer.usgs.gov), and the IMB catchment was delineated for computations to determine the slope factor (LS).

The *L*-factor was computed using Eq. 9 developed by Desmet and Govers (1996) while the *S*-factor was estimated using the McCool et al. (1987) method in Eq. 12.

$$L_{ij-\text{in}} = \frac{\left[\left(A_{i,J-\text{in}} + D^2 \right)^{m+1} - \left(A_{i,j-\text{in}} \right)^{m+1} \right]}{\left(D^{m+2} \right) \times \left(x_{i,j}{}^m \right) \times (22.13)^m} \quad (9)$$

$$m = \frac{\beta}{1+\beta} \quad (10)$$

$$\beta = \frac{\sin\theta / 0.0896}{3(\sin\theta)^{0.8} + 0.56} \quad (11)$$

$$S_{i,j} = \left\{ \begin{array}{l} 10.8 \sin\theta_{i,j} + 0.03, \, \tan\theta_{i,j} < 9\% \\ 16.8 \sin\theta_{i,j} - 0.50, \, \tan\theta_{i,j} \geq 9\% \end{array} \right\}, \quad (12)$$

where $L_{i,j-\text{in}}$ = slope length for grid cell (*i, j*); $A_{i,j-\text{in}}$ = contributing area at the inlet of the grid cell with coordinates (*i, j*) (m²); *D* = grid cell size (m); m = length exponent of the USLE *L*-factor; $x_{ij} = (\sin \alpha\, i, j + \cos \alpha\, i, j)$. β is the ratio of rill to inter-rill erosion for conditions when the soil is moderately susceptible to both rill and interrill erosion; θ is the slope angle in degrees (Oliveira 2015; Karamage et al. 2017). For efficiency, computing the LS-factor from the DEM of IMB catchment was accomplished using the ArcMap GISUS-M plugin (Oliveira 2015), whose LS Tool has inbuilt algorithms for automatically computing the LS factor from DEM (Oliveira 2015).

Cover-management factor (*C*)

C-factor represents the effect of ground and vegetation cover on the reduction of soil loss by reducing rainfall and runoff (Bekele and Gemi 2021). Land cover is the second most important factor next to topography controlling soil erosion risk (Uddin et al. 2016). The land cover intercepts rainfall, increases infiltration, and reduces rainfall energy. The IMB catchment land use map was generated in ArcGIS 10.5 software through supervised classification of a Landsat 8 satellite image of the IMB catchment downloaded from the USGS website (https://earthexplorer.usgs.gov), dated 12 December 2021. Averaged literature values for *C*-factors from similar studies in Sub-Saharan Africa were then assigned to particular land cover classes as illustrated in Table 2.

Support practice factor (*P*)

P-factor represents the impacts of support practices such as contouring or strip cropping on the erosion rate (Bekele and Gemi 2021; Panditharathne et al. 2019). Literature values for the *P*-factor, (Table 3) for the different land uses in IMB catchment were assigned to the land use Arc Map layer. The major crop cover was in the eastern catchment, which is relatively flat and hence the average *C*-factor for agricultural lands (0.5) (David 1988; Naqvi et al. 2012) was assigned and a 30 m resolution *P*-factor raster map for the catchment was generated.

Erosion risk

RUSLE predicted soil loss was categorized using the following thresholds: very slight, slight, moderate, high, severe and very severe, as shown in Table 4 (Bamutaze et al. 2021). The

Table 3 *P* values for the land use in IMB catchment

Land use/land cover classes	*P* value	Source
Agricultural cropland	0.5	David (1988), Naqvi et al. (2012)
All other land use except agricultural land	1	David (1988), Naqvi et al. (2012)

Table 4 Categories for RUSLE predicted soil loss

Code	Class	Erosion rate (t ha^{-1} year^{-1})
1	Very slight	<2
2	Slight	2–5
3	Moderate	5–10
4	High	10–50
5	Severe	50–100
6	Very severe	100–500

descriptive statistics encompassing the minimums, maximums, means, and standard deviations were obtained for each of RUSLE factors and the modelled erosion risk map. To envisage the spatial disparities of the input RUSLE layers and modelled erosion, mean and standard deviation values were utilised to compute the coefficients of variation (CV).

Field walks for identifying other erosion sources

The walks were centered on field observations to further understand the model results and identify other erosion hotspots other than those captured by the RUSLE model. As a recognized ecological monitoring tool, systematic walks (FAO 2015; Rojas and West 2021) and field investigations (Islam et al. 2020) were applied in this study to aid the further understanding of the erosion hotspots and sediment connectivity, given the complex drainage network of the IMB catchment in addition to the diverse land uses. The walk design was guided by the mapped erosion hotspots from the RUSLE model and the drainage network of the catchment since proximity to the drainage channels accelerates the transfer of the eroded soil downstream as sediment (Ali et al. 2021). Another consideration for these walks was accessibility, and therefore the road network was given utmost consideration, especially in the swampy and remote eastern part of the catchment. The map in Fig. 5 illustrates the field walks in the catchment.

Results

RUSLE factors

R-factor

The catchment exhibits a distinct rainfall erosivity gradient (Fig. 6) influenced by a wetter eastern side and gradually drying towards the west. The rainfall gradient directly correlates to the erosivity distribution. The *R*-factor results for the study area ranged from 665 to 874 MJ mm ha^{-1} h^{-1} year^{-1} (Fig. 6), with a mean value of 774 MJ mm ha^{-1} h^{-1} year^{-1}. The Zirimiti sub-catchment is shown to have the highest rainfall erosivity whereas the lowest erosivity was calculated for the Kansanga sub-basin. The Namanve sub-catchment is located in the transition between the high and low erosivity zones. With a standard deviation of 49 MJ mm ha^{-1} h^{-1} year^{-1}, the catchment had a low computed coefficient of variation (CV) for the *R*-factor of 6.33%.
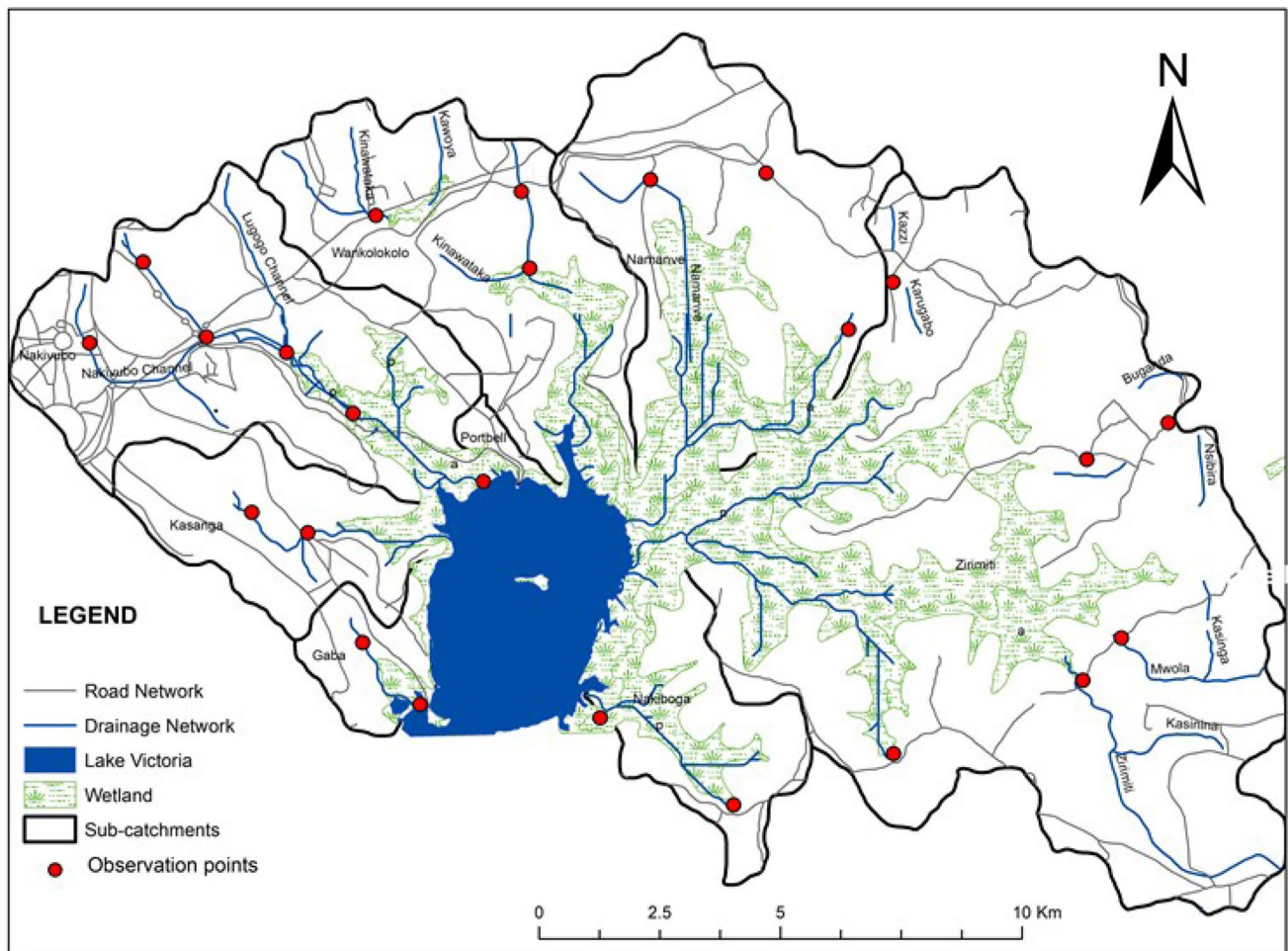
K-factor

The predominant soil types in IMB catchment are Gleysols and Ferralsols, covering 45.4% and 54.6% of the catchment area, respectively. Both soil types exhibited low erodibility values as per Institute for Water Resources, IWR (2002) erodibility classes (Table 1). The computed catchment *K*-factors ranged from a minimum of 0.018 to a maximum of 0.019 t ha h ha^{-1} MJ^{-1} mm^{-1} for Gleysols to Ferralsols respectively, as summarised in Table 5 and Fig. 7. The central catchment characterised by gleysols and lower erodibility, in contrast to the Western parts of Ggaba, Kansanga, Nakivubo and Kinawataka; Northern Namanve and Eastern Zirimiti sub-catchments (Fig. 7). The catchment erodibility had a mean value of 0.0185 t ha h ha^{-1} MJ^{-1} mm^{-1}, a standard deviation of 0.0007 and a coefficient of variation (CV) of 3.81%, signifying a low variation in erodibility of the catchment according to Bamutaze et al. (2021).

Slope length and steepness (LS-factor)

Computed LS-factor values ranged from as low as 0.01, shooting to a maximum of 30.5 for certain hills as shown in the map in Fig. 8. Spatially, the Western sub-catchment of Ggaba, Kansanga and Kinawataka exhibited high LS values. Central IMB catchment had the lowest LS-factors, attributed to the flat nature of the predominantly wetland central sub-catchments including Namanve, Nakiboga and

Fig. 5 Map showing the field walks in the IMB catchment

Western Zirimiti. The LS-factor eventually rises in the South Eastern Zirimiti sub-catchment (Fig. 8). LS-factor had a mean value of 1.33, a standard deviation of 1.93 and a coefficient of variation (CV) of 145.11%, thus portraying a high variance in the slope of the catchment.

### Cover-management (*C*-factor) and support practices (*P*-factor)

From the land cover map (Fig. 9), 23.2% of the area was built-up, 16.2% semi-built up (25–50% green), 8.6% forest area, 21.9% wetland cover, 28.1% cropland and 2% bare surfaces (bare soils). The western sub-catchments of Ggaba, Nakivubo, and Kinawataka were predominantly built-up, while the East was majorly covered with croplands. The central catchment is a transition from built-up to crop and forest cover, but also with a large wetland cover (Fig. 9). The *C*-factors in the catchment ranged from zero for open water and wetlands, to a maximum of 1 for bare surfaces (soils) (Fig. 9), as per assigned literature values in similar

Sub-Saharan Africa studies (Table 2). The cover factor of IMB catchment had a mean value of 0.131 and a standard deviation of 0.387.

Croplands comprised 28.1% of the IMB catchment area, while other land uses claimed 71.9% of the catchment area. Thus as per the guiding literature (Table 3), *P*-factor values ranged from 0.5 for agricultural croplands to 1 for other land uses (Fig. 9).

Erosion risk (RUSLE based)

RUSLE model results indicated the percentage catchment areas for the various erosion rates as; 66.7% for 0–2 t ha^{-1} year^{-1}, 10.8% for 2–5 t ha^{-1} year^{-1}, 10.1% for 5–10 t ha^{-1} year^{-1}, 9% for 10–50 t ha^{-1} year^{-1} and 3.3% for 50 and 100 t ha^{-1} year^{-1} erosion rates (Fig. 10). The average watershed erosion rate was 7 t ha^{-1} year^{-1}, ranging in moderate levels as per the guiding categorization in Table 4 (Bamutaze et al. 2021). Average erosion rates for the sub-catchments are summarized in Table 6.
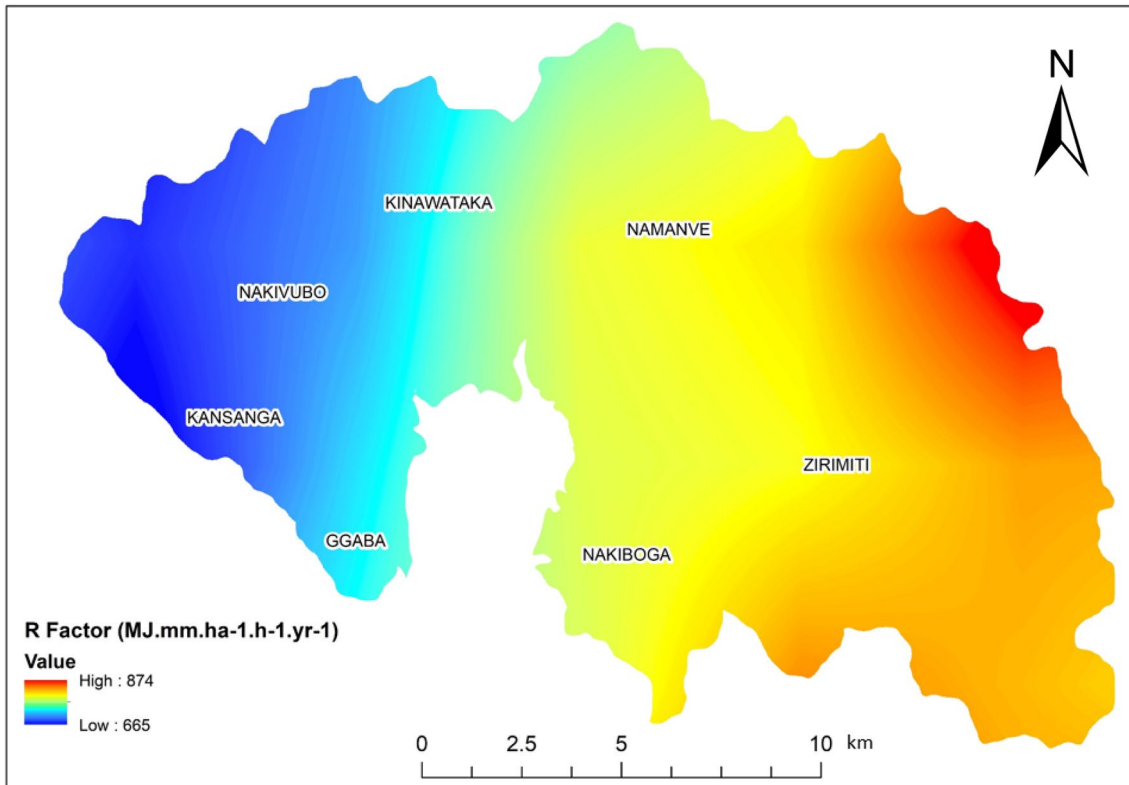
Fig. 6 The *R*-factor map for IMB catchment

Table 5 Calculated *K*-factor values

FAO soil type	Calculated *K*-factor (t ha h ha^{-1} MJ^{-1} mm^{-1})
Gleysols	0.018
Ferralsols	0.019

Major erosion sources

Prone zones: Generally, RUSLE predicted erosion-prone areas comprised of bare surfaces, croplands and steep areas (LS-factor > 20) as the major erosion hotspots (> 5 t ha^{-1} year^{-1}), with erosion rates up to 100 t ha^{-1} year^{-1} in a few worst case scenarios (Fig. 11).

Drainage channels: Field walks revealed that unlined drainage systems in the catchment are major erosion hotspots (Fig. 12), yet the RUSLE model does not consider that. Therefore, the modelled erosion values could be significantly higher than those reported from the RUSLE model, especially for several urban sub-catchments, given the high runoff values generated from the large paved surfaces.

Exposed/bare soils: Bare soils have increased erosion risks since the erosive energy of rainfall can detach and transport the soil particles with relative ease on such surfaces (Uddin et al. 2016). Such surfaces were very common in the sub-catchments and included: unpaved (marram/gravel roads), excavated areas, fresh developments/construction sites, football pitches, home compounds and exposed workspaces such as garages and parking spaces (Fig. 12).

Discussion

RUSLE factors

The increasing *R*-factor values eastwards of the IMB catchment are attributed to the higher rainfall values in the East (1570 mm) as compared to the Western side with rainfall lowering to 1198 mm. The attained *R*-factors in this study are comparable to results from similar studies in East and Central Africa in countries like Ethiopia, Kenya and the DRC (Bekele and Gemi 2021; Jothimani et al. 2022; Tsegaye and Bharti 2021; Njiru et al. 2018; Eisenberg and Fabrice 2020), where values ranged between 201 and 1066 MJ mm ha^{-1} h^{-1} year^{-1}. The computed *R* values were as well comparable to the ranges of EU Soil Data Centre (https://esdac.jrc.ec.europa.eu) global *R*-factors, where East African values generally range between 700 to 1700 MJ mm ha^{-1} h^{-1} year^{-1}.
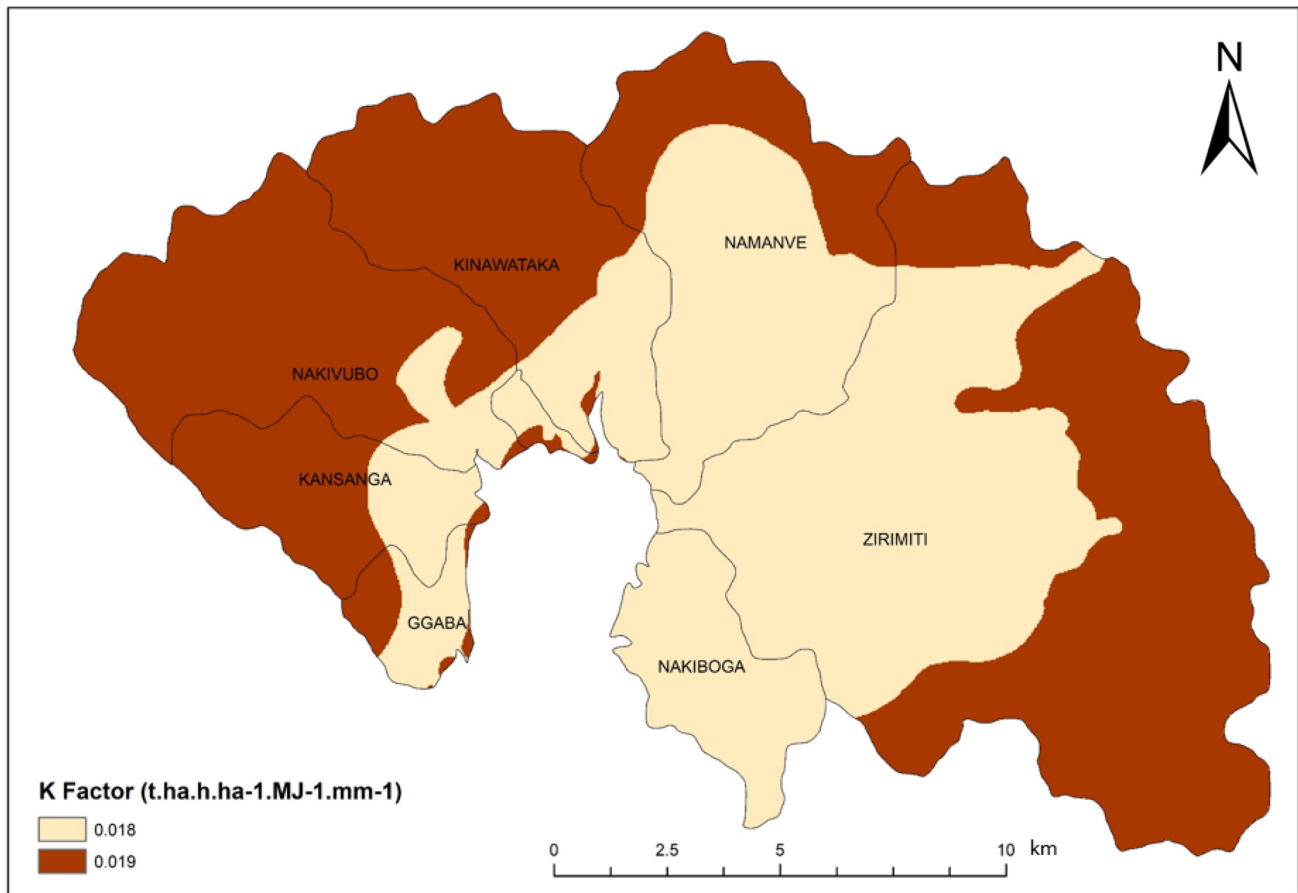
Fig. 7 *K*-factor map for IMB catchment soils

From the IWR (2002) classification as shown in Table 1. Low soil erodibility (0.006585–0.02634 t ha h ha^{-1} MJ^{-1} mm^{-1}) is for clay soils that are not easily detached or sandy soils that have a low runoff. Moderate erodibility (0.02634–0.05268 t ha h ha^{-1} MJ^{-1} mm^{-1}) signifies medium-textured soils, while high erodibility (> 0.05268 t ha h ha^{-1} MJ^{-1} mm^{-1}) denotes soils with high silt content and prone to more runoff and detachment. The spatial distribution of erodibility values is thus determined by the soil type, and with the predominant soil types in the IMB catchment being Gleysols and Ferralsols; both exhibited low erodibility, implying that the *K*-factor is not a major factor in the IMB catchment erosion risk, as compared to other RUSLE factors. For slope, the range of LS-factor is a reflection of the complex topographical variation from the West, Central to the East IMB catchment. Thus the high coefficient of variation (CV) of 145.11% is a representation of the heterogeneity in slopes within the catchment.

The spatial distribution of *C*-factors in the IMB catchment is a depiction of the underlying determinants, which are the different land uses and land covers. Since the eastern catchment was predominantly an agricultural area, it

exhibited the highest magnitude of *C*-factor (0.3), attributed to the susceptibility of croplands to erosion (Eisenberg and Fabrice 2020; Bamutaze et al. 2021; Marondedze and Schütt 2020). Nonetheless, significant forest cover in the eastern area can limit excessive erosion, hence a *C*-factor of 0.011 (Eisenberg and Fabrice 2020; Eniyew et al. 2021; Ligonja and Shrestha 2013; Tsegaye and Bharti 2021). Since the central IMB catchment was predominantly wetland covered, it reduces the erosion risk, thus the lowest *C*-factor (0), (Armour and Lait 2014; Rozos et al. 2013). The western catchment is majorly built-up, which reduces the soil exposure to detachment. Similar studies in Sub-Saharan Africa settings have highlighted such built-up and semi-built zones as low-prone areas to erosion although not necessarily resistant, with average *C* values of 0.035 and 0.11 for built-up and semi-built settings, respectively (Eisenberg and Fabrice 2020; Eniyew et al. 2021; Ligonja and Shrestha 2013; Marondedze and Schütt 2020). Non-agricultural land covered 71.9% of the IMB catchment with no agricultural erosion control practices where the *P*-factor for such areas is 1 (David 1988; Naqvi et al. 2012). The major crop cover being in
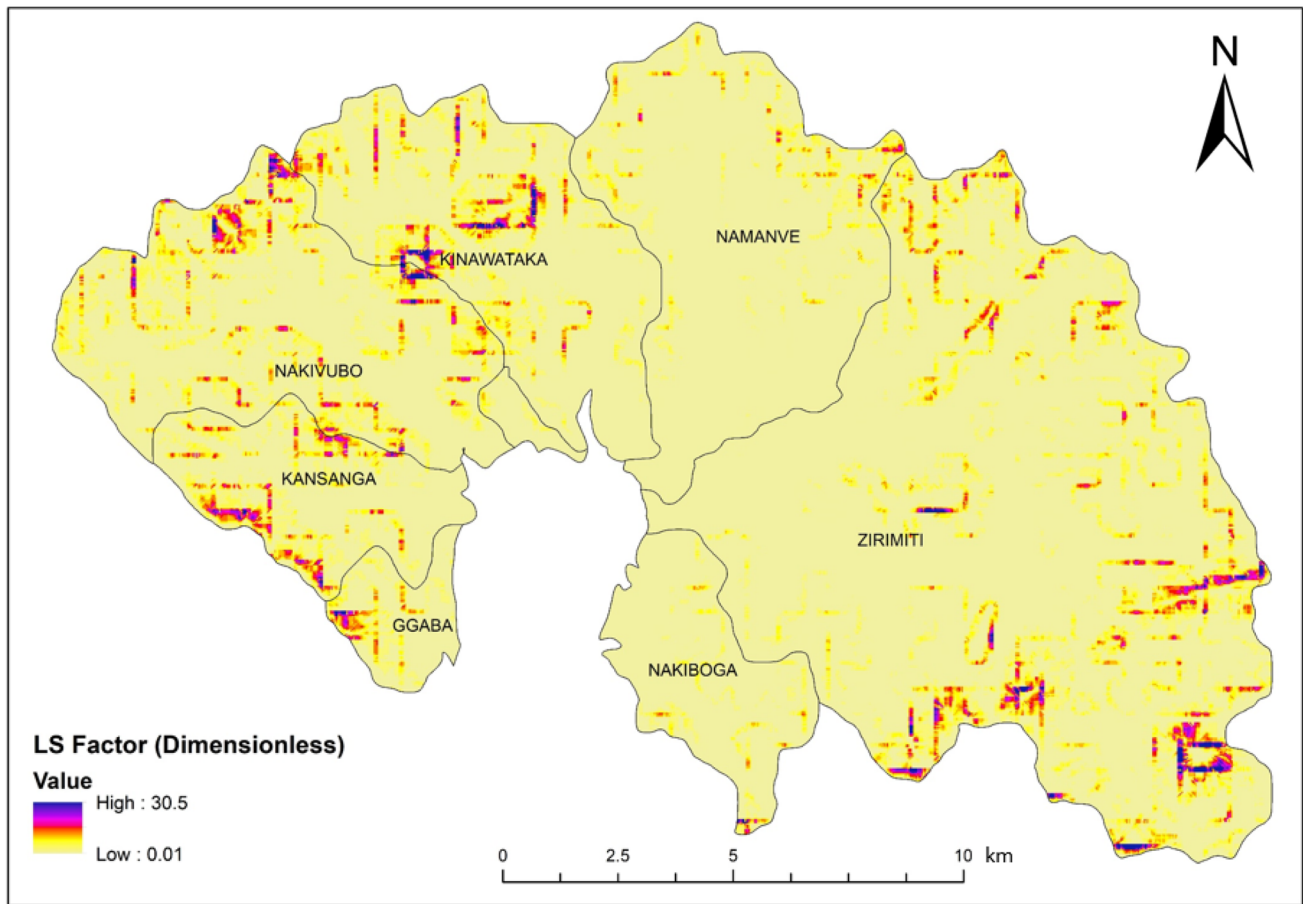
Fig. 8 LS-factor map for IMB catchment

the eastern catchment (Fig. 9), the average *C*-factor (0.5) for agricultural croplands (David 1988; Naqvi et al. 2012) was thus assigned.

Modelled erosion

RUSLE results exhibited a wide range of variations in erosion risk for the different sub-catchments of IMB watershed and according to Bamutaze et al. (2021), Uganda soil loss tolerance value is 5 t ha^{-1} year^{-1}. The erosion proneness of the Eastern catchment (Nakiboga and Zirimiti sub-catchments) was attributed to the higher rainfall values, with erosivity values surging as high as 871 MJ mm ha^{-1} h^{-1} year^{-1}. Furthermore, these sub-catchments are predominantly agricultural areas with high *C* values as compared to the urban western sub-catchments. RUSLE predicted erosion-prone areas in these eastern sub-catchments as croplands on the slopes, with erosion rates up to 100 t ha^{-1} year^{-1} in worst scenarios. However, the overall effect of this potential erosion on IMB ecological health is anticipated limited, as confirmed by the field walks. This is due to the large buffering effect of the

Zirimiti and Nakiboga wetlands in addition to the limited effluents in these rural sub-catchments. The middle catchment is relatively flat with LS-factor as low as 0.01, in addition to a predominant wetland cover whose *C*-factor is 0. This contributed to the lowest erosion risk in the central IMB catchment (Fig. 10).

Nonetheless, most western sub-catchments such as Nakivubo, Kansanga, Gaba (Kyetinda), Kinawataka, Portbell and Namanve are predominantly urban with most surfaces paved or semi-built up. RUSLE model calculated erosion risk with the soil *K* value cancelled out by the corresponding *C* value in such paved areas. However, these western sub-catchments are hilly with high LS-factors of up to 30.5. Thus in those catchments, RUSLE predicted higher erosion values on hills and semi-built up as well as agricultural areas in comparison to paved areas such as the Kampala city center. Predicted erosion-prone areas included Mbuya hill, Biina, Banda-Kyambogo, Kireka (Kiganda hill zone), Luzira farmlands and Makindye Lukuli (Fig. 11). Nevertheless, RUSLE modelled values for specific areas such as Kololo seemed slightly higher than the practical realities from field walks,
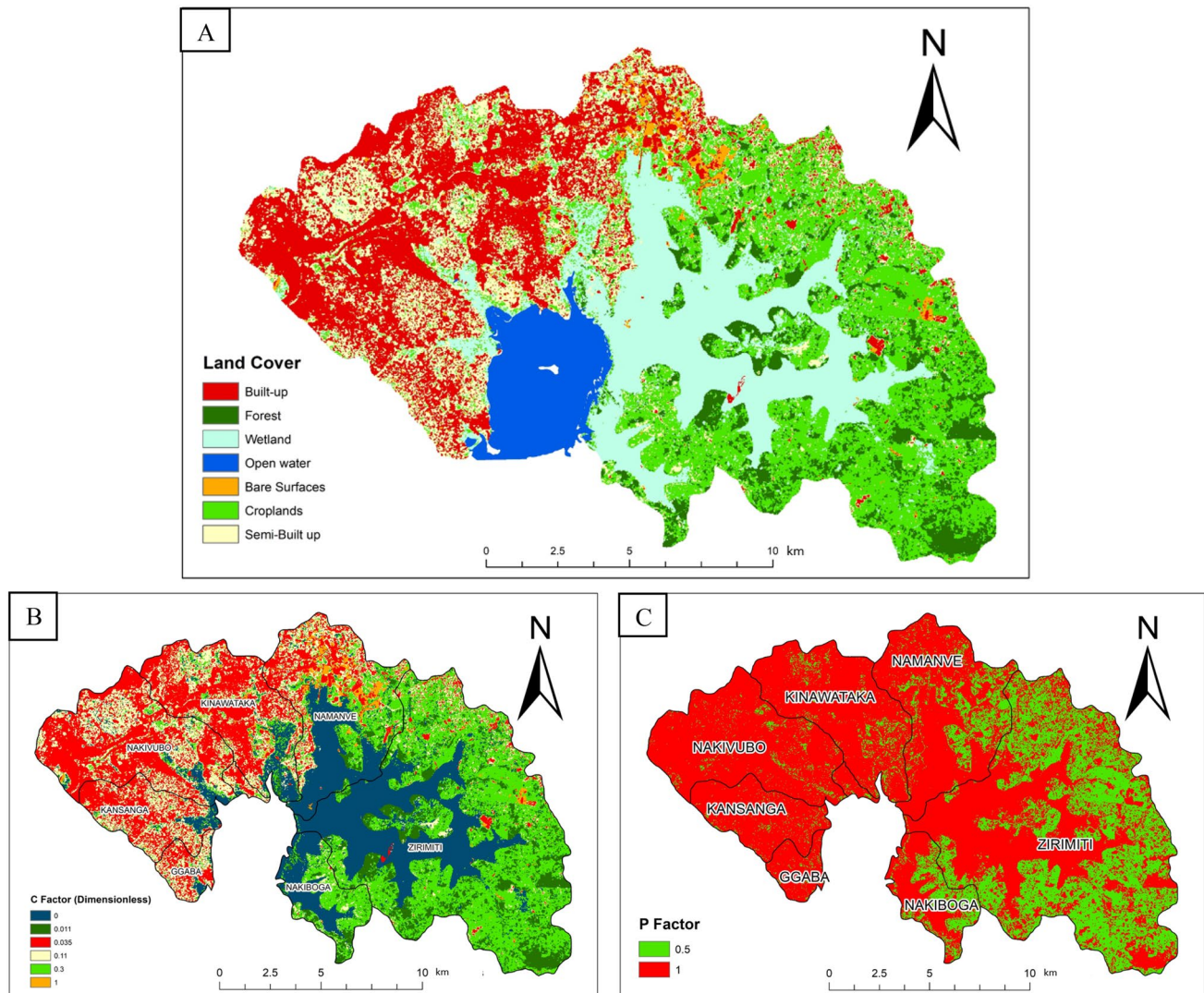
Fig. 9 a IMB catchment 2021 land use and cover map, **b** C-factor map for IMB catchment and **c** P-factor map for IMB catchment

attributed to their semi-built up and hilly nature with high LS-factor values.

Robust approaches were adhered to during modelling in this research and as a detachment model, RUSLE estimated the erosion risk with reliable results as confirmed from the field walks (Fig. 11). The field walks served a comparison purpose for further understanding of the RUSLE model results and ground realities as well as identification of other erosion hotspots than those captured by the model. Generally, most soil erosion studies in Sub-Sahara African countries including Uganda concentrated majorly on hilly (mountainous), agricultural areas as well as countryside catchments (Eisenberg and Fabrice 2020; Karamage et al. 2017; Tsegaye and Bharti 2021; Bamutaze et al. 2021), with minimum focus on urban and peri-urban settings. Karamage et al. (2017) conducted an erosion risk assessment in Uganda, identifying soil erosion hotspot areas that were

high priorities. RUSLE model predictions showed that the mean rate of soil loss risk in Uganda's erosion-prone lands was 3.2 t ha^{-1} year^{-1}, with a total annual soil loss of about 62 million tons in the year 2014. The study revealed that out of 112 Ugandan districts, 66 were found having unsustainable estimated soil loss rates > 1 t ha^{-1} year^{-1} (Karamage et al. 2017). Six districts were found to have mean annual soil loss rates of > 10 t ha^{-1} year^{-1} including Bududa (46.3 t ha^{-1} year^{-1}), Kasese (37.5 t ha^{-1} year^{-1}), Bundibugyo (28.9 t ha^{-1} year^{-1}), Bulambuli (20.9 t ha^{-1} year^{-1}), Sironko (14.6 t ha^{-1} year^{-1}) and Kotido (12.5 t ha^{-1} year^{-1}) (Karamage et al. 2017). In the findings, however, the estimated soil erosion risk categorised Kampala district and IMB catchment under non-erosive lands, attributed to its built-up and peri-urban nature. Thus, findings from Karamage et al. (2017) do not precisely align with the unveiled erosion threat in IMB catchment investigated further in this study.
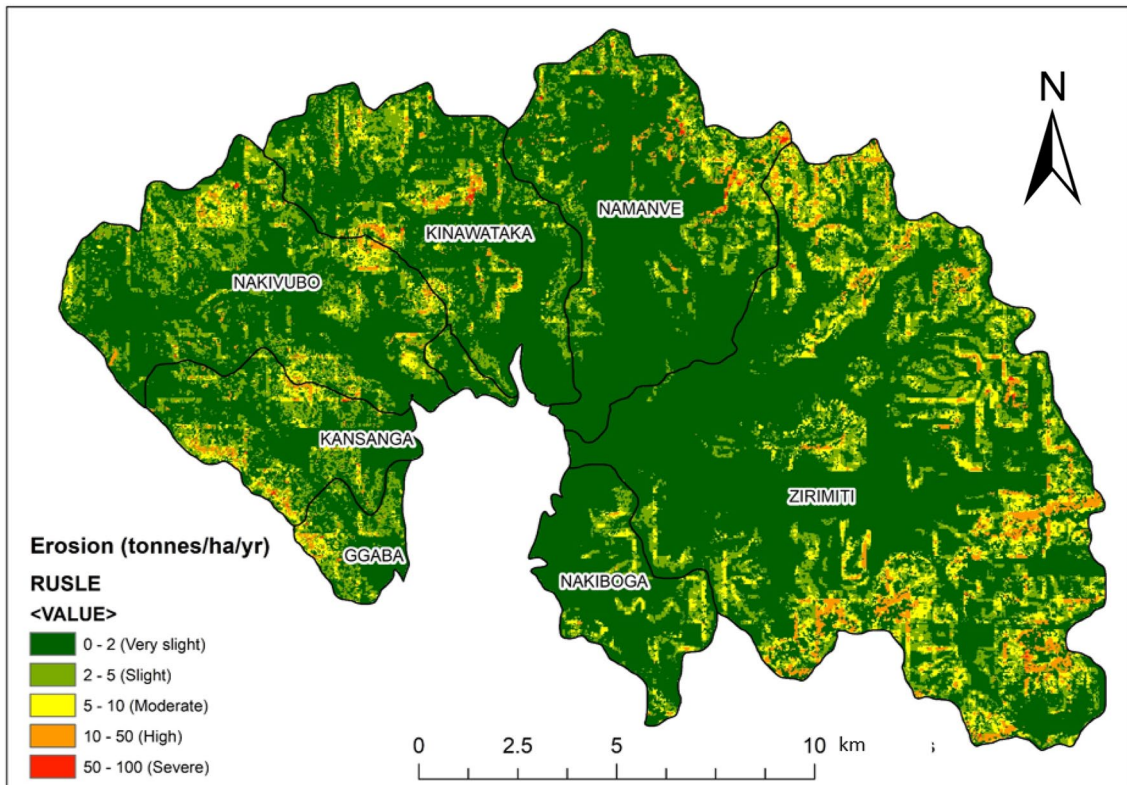
Fig. 10 IMB catchment modeled soil erosion by the RUSLE model

Though often regarded as non-erodible zones with significant portions of paved surfaces (Karamage et al. 2017), peri-urban catchments are associated with high runoff volumes and complex detachment mechanisms which instigate erosion and sediment transport (Marondedze and Schütt 2020). Globally, erosion risk assessments have majorly focused on agricultural and rural landscapes (Islam et al. 2020; Bekele and Gemi 2021; Wang et al. 2021), with RUSLE model application in peri-urban catchments not exhaustively investigated (Shikan-galah et al. 2016; Marondedze and Schütt 2020). From similar research in a peri-urban setting of Harare Metropolitan Province in Zimbabwe, 40% of the Epworth district was threatened

by increased soil erosion risk within the built-up areas leading to unsustainable soil loss (Marondedze and Schütt 2020). The predicted mean potential soil erosion rate was 13.2 t ha^{-1} year^{-1} between the years 1984–2018 and vulnerable areas to erosion were foot slope areas with direct tributaries to the major streams and steep sloping zones (Marondedze and Schütt 2020). Such erosion patterns from Marondedze and Schütt (2020), are in agreement with the findings of this study from an identical setting of IMB catchment. Findings from this research suggest that RUSLE model is applicable in peri-urban settings, with proper consideration of local catchment characteristics prior to the utilization of the model outputs. A high erosion risk from the catchment is a significant ecological threat to the ecosystem with sediment deposits alongside their adsorbed pollutants such as heavy metals, nutrients and micro-plastics (Banadda et al. 2009), posing grave health concerns to humans and the ecosystem flora and fauna. Literature findings from earlier studies confirm this increasing sedimentation of IMB and the deteriorating water quality in Lake Victoria as a whole (Bongomin 2011; Kayima et al. 2010; Banadda et al. 2009; Akurut et al. 2017; MWE 2018).

Table 6 Table showing the average erosion of each sub-catchment

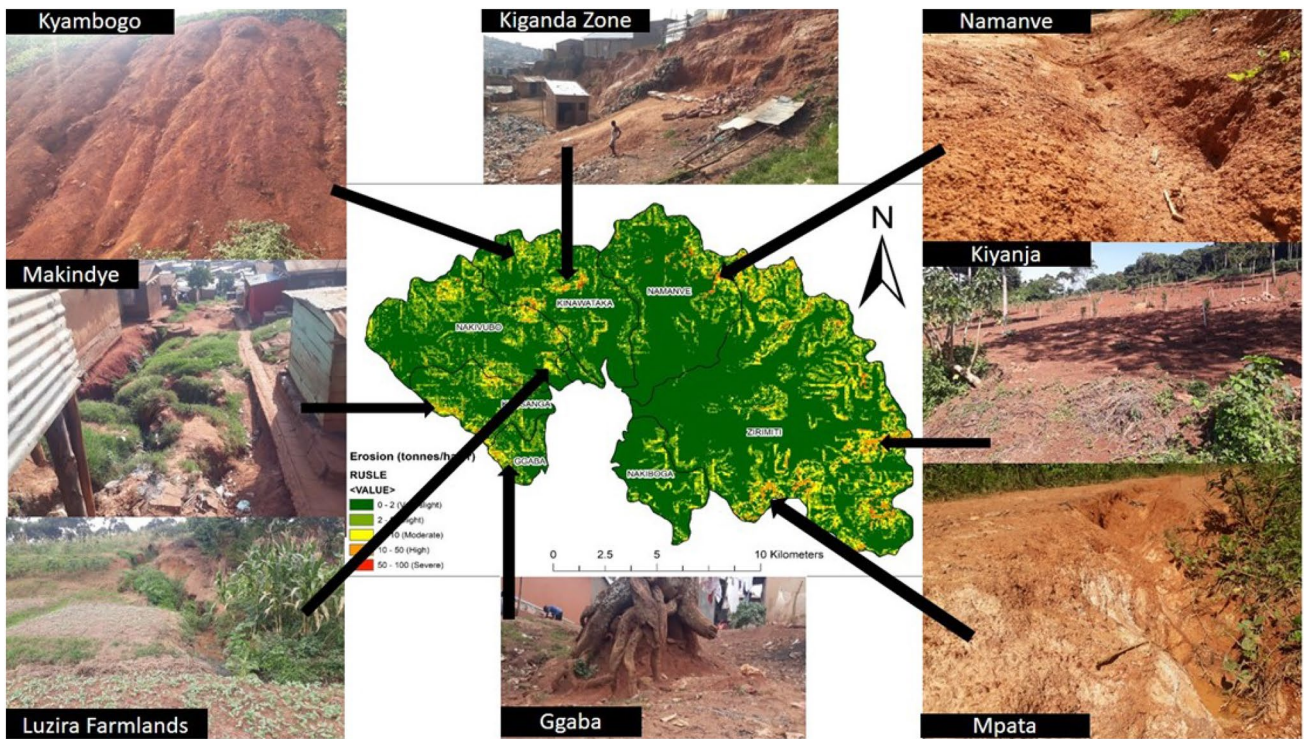| Sub-catchment	Average erosion rate (t ha^{-1} year^{-1})
Ggaba	7.5
Kansanga	7.1
Nakivubo	6.9
Kinawataka	7.8
Namanve	5.3
Zirimiti	9.4
Nakiboga	3.7

Fig. 11 Images from field walks for validating RUSLE predicted erosion-prone areas in IMB catchment

Fig. 12 Other identified erosion hot spots from field walks

Conclusions and recommendations

Results from this study unveiled a wide range of soil erosion hotspots, which are potential contributors to the overall sediment yield from the catchment into the Inner Murchison Bay (IMB) of Lake Victoria. The two ecological monitoring tools/approaches (RUSLE model and field walks) used in the catchment study unveiled unique attributes of erosion dynamics in the fragile IMB catchment. Where the RUSLE model identified croplands in hilly zones (LS-factor > 20) as the major erosion risk

hotspots (> 5 t ha^{-1} yr^{-1}), while the field walks identified bare surfaces, murram (gravel) roads and unlined drainage channels as other major erosion sources, especially in the semi-urban catchment. This serves as a basis for identifying mitigation priorities and its recommended that tailored soil and water conservation measures be integrated into physical planning, focusing on identified non-conventional hotspots to ameliorate sediment pollution in Lake Victoria. Nonetheless, this study encountered some limitations as some areas in the predominantly rural eastern catchment were not easily accessible due to the poor road network and multiple wetlands. Although RUSLE is regarded as the leading model in soil erosion risk assessment, further studies should focus on deploying multiple approaches in erosion mapping to envisage sediment connectivity and yield. Furthermore, the short temporal scales of erosion such as monthly or event basis were not addressed and should be studied more, since the annualized RUSLE erosion does not explicitly take it into consideration.

Data availability The datasets generated during and/or analysed during this study are available from the corresponding author upon reasonable request.

Declarations

Conflict of interest The authors declare that they have no conflict of interest.

References

AGLI. (2020). LAKE VICTORIA. https://www.africangreatlakesinform.org/article/lakevictoria#:~:text=The%20Lake%20Victoria%20basin%20is,250%20people%20per%20square%20km

Akurut M, Niwagaba CB, Willems P (2017) Long-term variations of water quality in the Inner Murchison Bay, Lake Victoria. Environ Monit Assess. https://doi.org/10.1007/s10661-016-5730-4

Ali MG, Ali S, Arshad RH, Nazeer A, Waqas MM, Waseem M, Aslam RA, Jehanzeb M, Cheema M, Leta MK, Shauket I (2021) Estimation of potential soil erosion and sediment yield: a case study of the transboundary chenab river catchment. water 13:3647. https://doi.org/10.3390/w13243647

Almasalmeh O, Saleh AA, Mourad KA (2022) Soil erosion and sediment transport modelling using hydrological models and remote sensing techniques in Wadi Billi, Egypt. Model Earth Syst Environ 8(1):1215–1226. https://doi.org/10.1007/s40808-021-01144-1

Anaba LA, Banadda N, Kiggundu N, Wanyama J, Engel B, Moriasi D (2017) Application of SWAT to assess the effects of land use change in the Murchison bay catchment in Uganda. Comput Water Energy Environ Eng 06(01):24–40. https://doi.org/10.4236/cweee.2017.61003

Armour JD, Lait R (2014) Catchment modelling of sediment, nitrogen and phosphorus nutrient loads with SedNet/ANNEX in the Tully–Murray basin. Mar Freshw Res. 60(11):1091–1096. https://doi.org/10.1071/MF08345

Bamutaze Y, Mukwaya P, Oyama S, Nadhomi D, Nsemire P (2021) Intersecting RUSLE modelled and farmers perceived soil erosion risk in the conservation domain on mountain Elgon in Uganda. Appl Geogr 126:102366. https://doi.org/10.1016/j.apgeog.2020.102366

Banadda EN, Kansiime F, Kigobe M, Kizza M, Nhapi I (2009) Landuse-based nonpoint source pollution: a threat to water quality in Murchison Bay, Uganda. Water Policy 11(SUPPL. 1):94–105. https://doi.org/10.2166/wp.2009.106

Bekele B, Gemi Y (2021) Soil erosion risk and sediment yield assessment with universal soil loss equation and GIS: in Dijo watershed, Rift valley Basin of Ethiopia. Model Earth Syst Environ 7(1):273–291. https://doi.org/10.1007/s40808-020-01017-z

Bongomin J. (2011) Modeling non-point source pollution in lake victoria: a case of gaba landing site, pp 32–48. https://www.mak.ac.ug/documents/Makfiles/theses/Bongomin%20Joachim.pdf

Clothier B (2015) Water: the world's most valuable natural asset. Integrated nutrient and water management for sustainable farming, 29, 11. http://flrc.massey.ac.nz/workshops/16/Manuscripts/Paper_Clothier_2016.pdf. Accessed 10 Sept 2021

David WP (1988) Soil and water conservation planning: policy issues and recommendations. J Philipp DevXV(1). https://core.ac.uk/download/pdf/6506014.pdf

Desmet PJJ. Govers G (1996) A GIS procedure for automatically calculating the USLE LS factor on topographically complex landscape units. J Soil Water Conserv 51:427–433

Eisenberg J, Fabrice MA (2020) Quantification of erosion in selected catchment areas of the Ruzizi River (DRC) using the (R)USLE Model. Land 9(4):125. https://doi.org/10.3390/land9040125

Eniyew S, Teshome M, Sisay E, Bezabih T (2021) Integrating RUSLE model with remote sensing and GIS for evaluation soil erosion in Telkwonz Watershed, Northwestern Ethiopia. Remote Sens Appl Soc Environ 24(September):100623. https://doi.org/10.1016/j.rsase.2021.100623

FAO (2015). Reconnaissance visit and transect walk.http://www.fao.org/fileadmin/templates/nr/kagera/Documents/LADA_manuals/part2_b.pdf.

FAO. (2019). Soil erosion. the greatest challenge for sustainable soil management. https://www.fao.org/3/ca4395en/ca4395en.pdf

Ganasri BP, Ramesh H (2016) Assessment of soil erosion by RUSLE model using remote sensing and GIS—a case study of Nethravathi Basin. Geosci Front 7(6):953–961. https://doi.org/10.1016/j.gsf.2015.10.007

Haande S, Rohrlack T, Semyalo RP, Brettum P, Edvardsen B, Lyche-Solheim A, Sørensen K, Larsson P (2011) Phytoplankton dynamics and cyanobacterial dominance in Murchison Bay of Lake Victoria (Uganda) in relation to environmental conditions. Limnologica 41(1):20–29. https://doi.org/10.1016/j.limno.2010.04.001

Huang Z, Liu C, Zhao X, Dong J, Zheng B (2020) Risk assessment of heavy metals in the surface sediment at the drinking water source of the Xiangjiang River in South China. Environ Sci Europe. https://doi.org/10.1186/s12302-020-00305-w

Hurni H (1985) Soil conservation manual for Ethiopia. First draft. Ministry of Agriculture, Natural Resources Conservation and Development Department, Community Forests and Soil Conservation Development Department, Addis Ababa

Islam A, Sarkar B, Das BC, Barman SD (2020) Assessing gully asymmetry based on cross-sectional morphology: a case of Gangani Badland of West Bengal, India. In: Gully erosion studies from India and surrounding regions. Springer, Cham, pp 69–92. https://doi.org/10.1007/978-3-030-23243-6_5

IWR (2002) Technical guide to RUSLE use in Michigan: RUSLE online soil erosion tool, vol 2020. IWR

Jaishankar M, Tseten T, Anbalagan N, Mathew BB, Beeregowda KN (2014) Toxicity, mechanism and health effects of some heavy metals. Interdiscip Toxicol 7(2):60–72. https://doi.org/10.2478/intox-2014-0009

Jothimani M, Getahun E, Abebe A (2022) Remote sensing, GIS, and RUSLE in soil loss estimation in the Kulfo river catchment, Rift valley, Southern Ethiopia. J Degrad Min Land Manag. https://doi.org/10.1524/jdmlm.2022.092.3307

Karamage F, Zhang C, Liu T, Maganda A, Isabwe A (2017) Soil erosion risk assessment in Uganda. Forests. https://doi.org/10.3390/f8020052

Kayima J, Kyakula M, Komakech W, Echimu S (2010) A study of the degree of pollution in Nakivubo Channel, Kampala, Uganda. J Appl Sci Environ Manag. https://doi.org/10.4314/jasem.v12i2.55540

Kolding J, Mkumbo OC, Zwieten PAM, Van (2014) Status, trends and management of the lake victoria fisheries. FAO fisheries and aquaculture technical paper 579. In press. https://www.academia.edu/6346054/Status_trends_and_management_of_the_Lake_Victoria_Fisheries

Lake Victoria Environment Management Programme (2005) Lake victoria environment report—Uganda water quality and ecosystems status. December, 1–36

Ligonja PJ, Shrestha R (2013) Soil erosion assessment in kondoa eroded area in Tanzania using universal soil loss equation, geographic information systems and socioeconomic approach. Land Degrad Dev. https://doi.org/10.1002/ldr.2215

Marondedze MAK, Schütt B (2020) Assessment of soil erosion using the RUSLE model for the Epworth district of the Harare Metropolitan province, Zimbabwe. Sustainability 12(20):8531. https://doi.org/10.3390/su12208531

McCool DK, Brown LC, Foster GR, Mutchler CK, Meyer LD (1987) Revised slope steepness factor for the universal soil loss equation. Trans ASAE 30:1387–1397

Mekonnen M, Melesse AM (2011) Soil erosion mapping and hotspot area identification using GIS and remotesensing in northwest ethiopian highlands, near lake tana. Nile River Basin; hydrology, climate & water use,Springer, pp 207–224

Ministry of Water and Environment (2018) Water and environment sector performance report 2018. https://www.mwe.go.ug/library/sector-performance-report-2018

Naqvi HR, Mallick J, Devi LM, Siddiqui MA (2012) Multi-temporal annual soil loss risk mapping employing revised universal soil loss equation (RUSLE) model in nun nadi watershed, Uttrakhand (India). Arab J Geosci 6:4045–4056 (2013). https://doi.org/10.1007/s12517-012-0661-z

Njiru G, Kariuki P.Mwetu K (2018) Modelling soil erosion for land management in ungauged golole catchment in marsabit county, Kenya. Open J Soil Sci 8:277–302. https://doi.org/10.4236/ojss.2018.811021

Oliveira J (2015) A GIS-based procedure for automatically calculating soil loss from the universal soil loss equation: GISus-M. Appl Eng Agric 31(6):907–917. https://doi.org/10.13031/aea.31.11093

Panditharathne DLD, Abeysingha NS, Nirmanee KGS, Mallawatantri A (2019) Application of revised universal soil loss equation (Rusle) model to assess soil erosion in "kalu Ganga" River Basin in Sri Lanka. Appl Environ Soil Sci. https://doi.org/10.1155/2019/4037379

Renard KG, Foster GR, Weesies DK, Yoder DC (1997) Predicting soil loss by water: a guide to conservation planning with the revised soil loss equation (RUSLE). US Department of Agriculture, no. 2, Washington DC, USA, pp 11–23

Rojas BA, West CT (2021) Walking the line: conducting transect walks in Burkina FASO. Pract Anthropol 43(1):18–21. https://doi.org/10.17730/0888-4552.43.1.18

Rozos DE, Loupasakis C, Hariklia DS, George D (2013) Application of the revised universal soil loss equation model on landslide prevention. An example from N. Euboea (Evia) Island. Greece. Environ Earth Sci 70:3255–3266. https://doi.org/10.1007/s12665-013-2390-3

Sankhla MS, Kumari M, Nandan M, Kumar R, Agrawal P (2019) Heavy metals contamination in water and their hazardous effect on human health—a review. SSRN Electron J 5(10):759–766. https://doi.org/10.2139/ssrn.3428216

Shikangalah RN, Florian J, Niels B, Eve NM (2016) A review on urban soil water erosion. J Stud Hum Soc Sci 5(1):163–178. https://journals.unam.edu.na/index.php/JSHSS/article/view/1033

Ssebiyonga N, Erga SR, Hamre B, Stamnes JJ, Frette Ø (2013) Light conditions and photosynthetic efficiency of phytoplankton in Murchison Bay, Lake Victoria, Uganda. Limnologica 43(3):185–193. https://doi.org/10.1016/j.limno.2012.09.005

Tamene L, Adimassu Z, Ellison J, Yaekob T, Woldearegay K, Mekonnen K, Thorne P, Le QB (2017) Mapping soil erosion hotspots and assessing the potential impacts of land management practices in the highlands of Ethiopia. Geomorphology 292:153–163. https://doi.org/10.1016/j.geomorph.2017.04.038

Tamene L, Le QB (2015) Estimating soil erosion in sub-saharan africa based on landscape similarity mapping and using the revised universal soil loss equation (RUSLE). Nutr Cycl Agroecosyst 102:17–31. https://doi.org/10.1007/s10705-015-9674-9

Tebandeke IZM, Karume I, Wasajja HZ, Nankinga R (2020) Improving quality of water from murchison bay using clay from chelel, Kapchorwa district, Ugandao. J Of Adv Chem, 17, 1–29.https://doi.org/10.24297/jac.v17i.8537

Tsegaye L, Bharti R (2021) Soil erosion and sediment yield assessment using RUSLE and GIS-based approach in Anjeb watershed, Northwest Ethiopia. SN Appl Sci 3(5):1–19. https://doi.org/10.1007/s42452-021-04564-x

Uddin K, Murthy MSR, Wahid SM, Matin MA (2016) Estimation of soil erosion dynamics in the koshi basin using GIS and remote sensing to assess priority areas for conservation. PLoS ONE. https://doi.org/10.1371/journal.pone.0150494

UNCCD (2017) Global land outlook, 1st edn

UNITED NATIONS (2016) Transforming our world: the 2030 agenda for sustainable development. sustainabledevelopment.un.org

Wang R, Zhang S, Yang J, Yang C (2016) Integrated use of GCM, RS, and GIS for the assessment of hillslope and gully erosion in the Mushi River sub-catchment, Northeast China. Sustainability. https://doi.org/10.3390/su8040317

Wang JY, Zhu YQ, Chen PF (2021) Methodology for 1-km raster dataset of annual. J Glob Change Data Discov 5(1):54–61. https://doi.org/10.3974/geodp.2021.01.07

Wischmeier WH, Smith DD (1978) Predicting rainfall erosion losses. a guide to conservation planning supersedes agriculture handbook no. 282